

Y. Aa, Z. H. Cao, Z. M. Tang, Z. W. Sun and W. R. Hu

Experimental Study on the Transition Process to the Oscillatory Thermocapillary Convections in a Floating Half Zone

The transition process of the thermocapillary convection from a steady and axisymmetric mode to the oscillatory mode in a liquid bridge with a fixed aspect ratio and varied volume ratio was studied experimentally. To ensure the surface tension to play an important role in the ground-based experiment, the geometrical configuration of the liquid bridge was so designed that the associated dynamic Bond number $B_d \approx 1$. The velocity fields were measured by Particle Image Velocimetry (PIV) technique to effectively distinguish the different flow modes during the transition period in the experiments. Our experiments showed that as the temperature difference increased the slender and fat bridges presented quite different features on the evolution in their flow feature: for the former the thermocapillary convection transformed from a steady and axisymmetric pattern directly into an oscillatory one; but for the latter a transition flow status, characterized by an axial asymmetric steady convection, appeared before reaching the oscillatory mode. Experimental observations agree with the results of numerical simulations and it is obvious that the volume of liquid bridge is a sensitive geometric parameter. In addition, at the initial stage of the oscillation, for the former a rotating oscillatory convection with azimuthal wave number $m = 1$ was observed while for the latter a pulsating oscillatory pattern with azimuthal wave number $m = 2$ emerged, and then with further increase of the temperature difference, the pulsating oscillatory convection with azimuthal wave number $m = 2$ evolved into a rotating oscillatory pattern with azimuthal wave number $m = 2$.

1 Introduction

Thermocapillary convection driven by a surface tension gradient along a free surface has attracted much interest because of its importance in the applications in crystal growth techniques such as the floating zone processing and the theoretical mechanism of a typical flow system in conditions of both earth gravity and microgravity environments. The liquid bridge model of floating half zone, simplified from the floating zone, is a typical model for studying thermocapillary convection. The floating half zone forms a liquid bridge held between two solid disks at different temperatures. Transition from steady and axisymmetric thermocapillary convection to oscillatory thermocapillary convection (OTC) occurs when the temperature difference in a floating half zone exceeds the critical value. The experiments for a large Prandtl number liquid bridge show that the critical temperature difference for the onset of OTC depends strongly on the volume of the liquid bridge [1-5]. Two different oscillatory branches were found with respect to the variation of the liquid bridge volumes, and the features related to these two branches are designated as the slender liquid bridges and the fat liquid bridges. There is a small range of volumes between these two oscillatory branches, where the critical Marangoni number is relatively large [1, 6-7]. Numerical simulation and energy method are used to explain such experimental results [5, 8].

In the earlier studies with right cylindrical liquid bridges of large Prandtl number fluids, thermocapillary convection was often thought to transform directly from a steady and axisymmetric mode to oscillatory mode [9-17]. A mechanism for the onset of such oscillation is suggested as the hydrothermal instability characterized by traveling waves [18]. There are two bifurcation transitions, firstly from a steady and axisymmetric convection to a steady and three-dimensional convection, and then from a steady and three-dimensional convection to oscillatory convection for small Prandtl number fluids (the order of magnitude of $Pr \approx 0.01$) [19-20]. For the two bifurcation transitions, the mechanism for the onset of oscillation is the hydrodynamic instability, which is different from the hydrothermal instability. Recently, numerical simulations for a 10cst silicone

Mail Address:

National Microgravity Laboratory / CAS, Institute of Mechanics,
Chinese Academy of Sciences, No. 15 Beisihuanxi Road, Beijing 100080, China

Paper submitted:
Submission of final revised Version:
Paper finally accepted:

oil liquid bridge of a larger Prandtl number ($Pr = 105.6$) reached similar conclusions as for small Prandtl number ($Pr = 0.01$) in both microgravity environments [21] and earth gravity condition [22]. For the slender liquid bridge the steady and axisymmetric thermocapillary convection transforms directly to OTC, but for the fat liquid bridge it transforms to OTC via the steady and axial asymmetric mode. Linear instability analysis gives the first bifurcation from a steady and axisymmetric convection to OTC for the slender liquid bridge; and to a steady and asymmetric convection for the fat liquid bridge [23]. All conclusions related to two bifurcation transitions were predicted only by theoretical approach and there has no experimental verification reported yet. As a matter of fact, Frank and Schwabe, based on their experimental observation, have noticed the time-independent but three-dimensional flow states and mentioned, "The broken symmetry was probably affected by a hydrodynamical instability" [24]. We have been using "axial asymmetric flow" to describe the three-dimensional flow.

The motivation of the present study is to verify experimentally whether and under what condition such two bifurcation transitions exist. The key problem for the experimental verification is how to effectively distinguish the transition of time-independent convections from the axisymmetric mode to the asymmetric mode. The difference appeared between the axisymmetric and asymmetric convections were not so obviously observable. It would be desirable to obtain the temperature field (or distribution) over a cross section of the liquid bridge. However, to our knowledge, there is no general way to measure the temperature field inside a liquid bridge. It is only possible to measure the temperatures at limited few points. We used thermocouples to measure temperature but could not put too many thermocouples into the liquid bridge. Therefore we could gain information about the temperature distribution only at some particular points instead of a temperature field over a cross section in the liquid bridge. Diagnosis of the temperature differences at two symmetric locations (for instance, at the two ends of a diameter) in the flow field seems a simple way to detect the asymmetry of the flow. In practice, however, there are some difficulties to catch such temperature differences. For one thing, it is hard to insert thermocouples into fluid at desired symmetric locations (at the two ends of a diameter of one of the

concentric circles - the original isotherms) with sufficient accuracy considering only tiny temperature difference (the maximum temperature difference, over all concentric circles in an entire horizontal cross-section, would be less than $0.2\text{ }^\circ\text{C}$, according to the numerical simulation of [21]) caused the asymmetry of the convection exists. In addition, whenever the asymmetric convection turns up, the orientation of its asymmetry (the maximum temperature difference would be along this direction) is unpredictable so we could not know where to put the thermocouples to effectively distinguish the temperature difference. Actually, to the best of our knowledge measurement of two-dimensional temperature field (not just points) inside fluid is impracticable. Although images of fluid flow, with the aid of tracers, can provide a view of the flow pattern to some extent, they are not sufficient to distinguish detailed changes in flow characteristics. More specifically, the images snapped during fluid motion basically can show only the trajectories of each tracer in fluid not the motion tendency of them.

On the other hand, flow field mapping depicting quantitatively velocity distribution of a fluid carries much more information (namely, showing the motion tendencies - the magnitudes and the directions, of the tracers) on flow features and therefore is a more powerful to detect changes in characteristics of thermocapillary convections. In this study, the Particle Image Velocimetry (PIV) was adopted to provide the velocity field in a horizontal cross-section of the liquid bridge while the temperature difference was increased.

The present paper presents direct experimental evidence showing the onset of OTC via two bifurcations for fat liquid bridges and one bifurcation for slender liquid bridges.

A liquid bridge has mainly two typical geometrical parameters: the geometrical aspect ratio $A = \lambda/d_0$ and volume ratio V/V_0 , where λ and d_0 are, respectively, the height of the liquid bridge and the diameter of the solid disk, V and V_0 are, respectively, the volume of liquid bridge and the volume of a right circular cylinder ($V_0 = \pi\lambda d_0^2/4$). Many studies suggest that m depends on only the aspect ratio $A = \lambda/d_0$ [25-29], and wave number m represents the number of cycles in the azimuthal direction and relates to OTC flow structure. The present paper shows that m depends not only on the aspect ratio $A = \lambda/d_0$ but also on the ratio of the liquid bridge volume V/V_0 . This paper also shows that OTC starts as a "rotating" mode $m = 1$ for a slender liquid bridge ($V/V_0 = 0.8$), and as a "pulsating" mode $m = 2$ for a fat liquid bridge ($V/V_0 = 0.985$).

2. Experimental methods

10cst silicone oil was used as experimental liquid. All experiments were performed under the room temperature around 23°C . The liquid bridge was floated in the gap between two coaxial solid circular disks having the same diameter $d_0 = 5\text{ mm}$ with a tolerance of $\pm 0.01\text{ mm}$. The distance between the top and bottom disks (height of the liquid bridge) was $2.5 \pm 0.01\text{ mm}$.

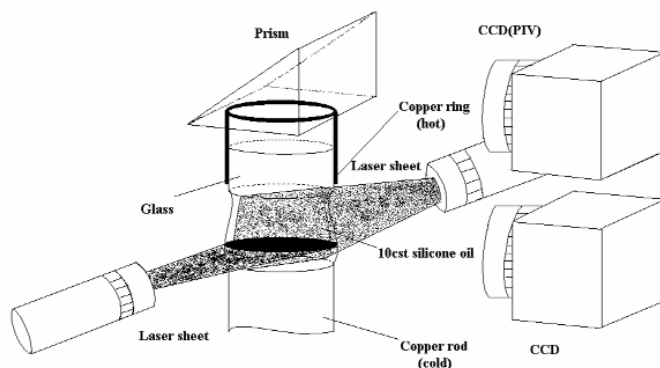


Fig. 1. Schematic of experimental facility.

The alignment of the centers of two disks was carefully done under a video monitor. We assume the liquid bridge held between two disks should be in a satisfactorily axisymmetric geometry because steady and asymmetric convections did not show any preferable orientation in all our experiments.

Fig. 1 shows the schematic of the experimental facility. The lower disk consists of copper; the upper disk is transparent glass K9 heated by an electrical resistance. The transparency of upper disk permits flow visualization and PIV measurement in a horizontal cross-section of the liquid bridge. Temperatures were measured by thermocouples on the sides of the solid disks that face the liquid bridge. A PID-controller (EUROTHERM 904 controller) controlled heating rate and temperature difference between the upper and lower disk.

A Flowmap PIV system (Dantec Measurement Technology A/S) was used to measure quantitatively velocity distribution of flow field in a horizontal cross-section of the liquid bridge. Particles (hollow glass spheres of density $\rho = 1.1 \text{ g/cm}^3$) of $10 \text{ }\mu\text{m}$ in mean diameter were suspended as tracers in the liquid bridge. Densities of tracer particles and 10cst silicone oil ($\rho = 0.94 \text{ g/cm}^3$) are close. The horizontal cross-section of the liquid bridge was illuminated by a light sheet of 0.3 mm thickness, which was produced by an argon ion laser (1.0 W). Another light sheet produced by a He-Ne laser (5mW) was applied to a vertical cross-section of the liquid bridge. An 80C42 DoubleImage 700 camera recorded the PIV pictures. The illumination system and camera were controlled automatically by a synchronization board in the PIV 2000 processor which processed images into vectors and displayed the results in real-time. Vector map acquisitions at the frequency of 15 Hz made it

possible to find whether the flow field in the liquid bridge was steady or not.

The accuracy and reliability of the system on Dantec Measurement Technology A/S were discussed elsewhere [30]. Calibration and validation of the experimental technique were given by a velocity model with input parameters in both the direction and the magnitude at certain flow points in a liquid bridge, and has been discussed elsewhere [31]. The accuracy of measured velocity was about 5%.

Based on previous theoretical analyses, bifurcation features should depend on the volume of liquid bridge, which is an essentially critical parameter [21-23]. The volume of the liquid bridge was evaluated by using a measuring system consisting of a CCD camera and a computer with an image-acquiring card. A special code for image processing was used to define the bound-

Fluid	Silicone oil 10 (cst)
$\rho \text{ (kg/m}^3\text{)}$	0.935×10^3
$\sigma_T \text{ (kg/s}^2\text{.}^\circ\text{C)}$	-0.6×10^{-4}
$\nu \text{ (m}^2\text{/s)}$	1×10^{-5}
$\kappa \text{ (m}^2\text{/s)}$	9.47×10^{-5}
$\beta \text{ (1/}^\circ\text{C)}$	1.08×10^{-3}
$g \text{ (m/s}^2\text{)}$	9.8

Table 1. Fluids properties used in the experiments and the calculations

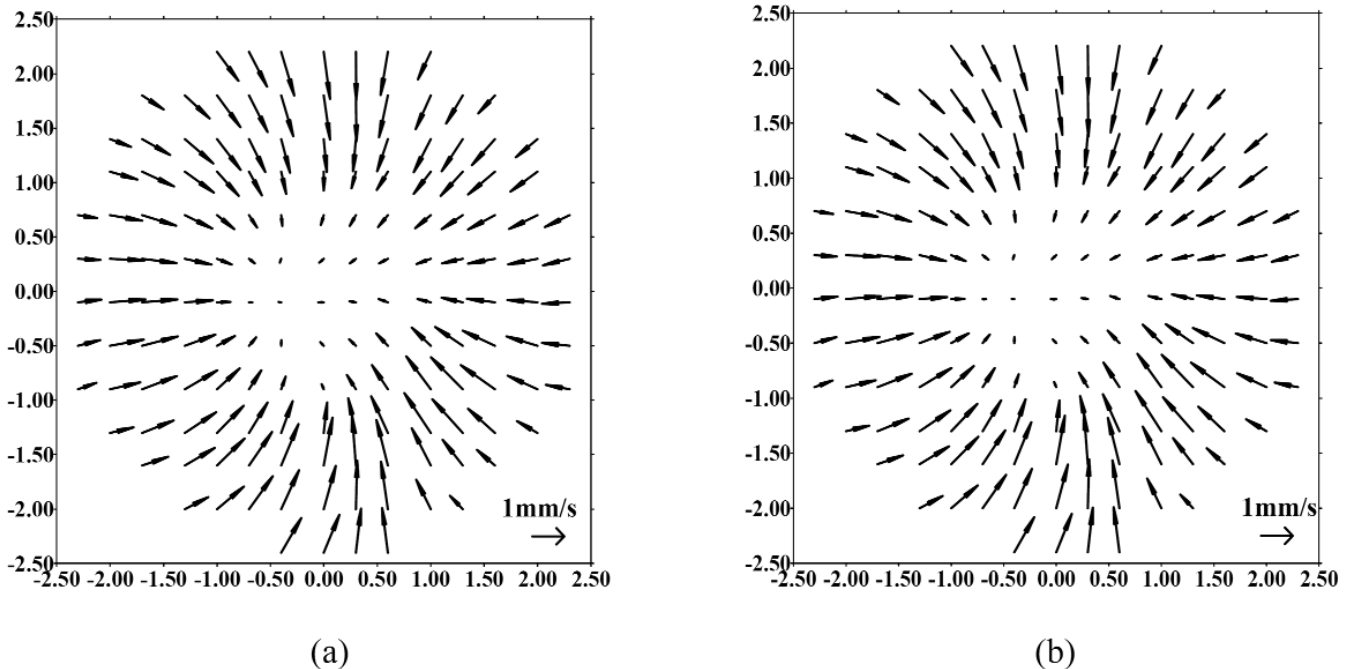


Fig. 2. Steady and axial asymmetric distribution of velocity in the horizontal cross-section ($z/\lambda = 0.25$) of a fat liquid bridge ($V/V_0 = 0.985$) at different time when temperature difference keeps at $\Delta T = 28^\circ\text{C}$ (a) $t = t_0$, (b) $t = t_0 + 120 \text{ second}$.

aries of the liquid bridge.

Dynamic Bond number $B_d = \rho g \lambda^2 \beta / |\sigma_T|$ measures relative importance between the gravity effect and the thermocapillary effect, where g is the acceleration of gravity, ρ , β and σ are, respectively, the density, thermal expansion coefficient and surface tension of the liquid, and σ_T is the partial derivative of surface tension with respect to temperature, the values of these fluid properties are given in table 1. In the present experiments, aspect ratio $A = \lambda/d_0 = 0.5$ and dynamic Bond number $B_d \approx 1$, which suggests that thermocapillary effect was the significant factor compared with gravity effect.

3 Transition Process in a Fat Liquid Bridge

During the experiments, temperature difference ΔT was increased with a rate of 4.0 °C/minute, and then kept constant by the PID-controller when the velocity distributions were

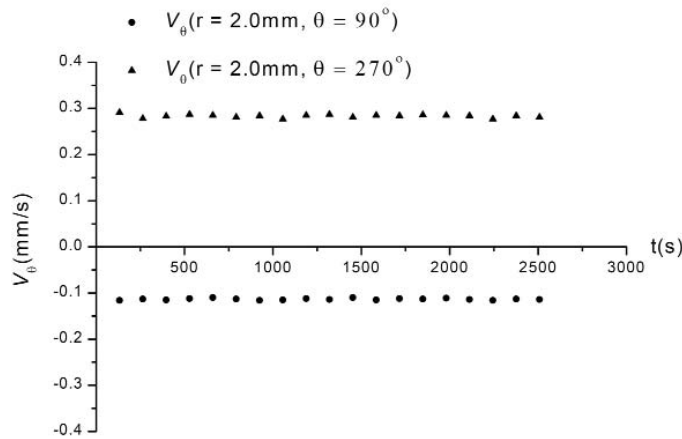


Fig. 3. A graph for the variation of azimuthal velocity components with time at two fixed points ($r = 2.1 \text{ mm}$, $\theta = 90^\circ$ and $\theta = 270^\circ$) of flow field in the horizontal cross-section ($z/\lambda = 0.25$) of liquid bridge when temperature difference $\Delta T = 22^\circ\text{C}$.

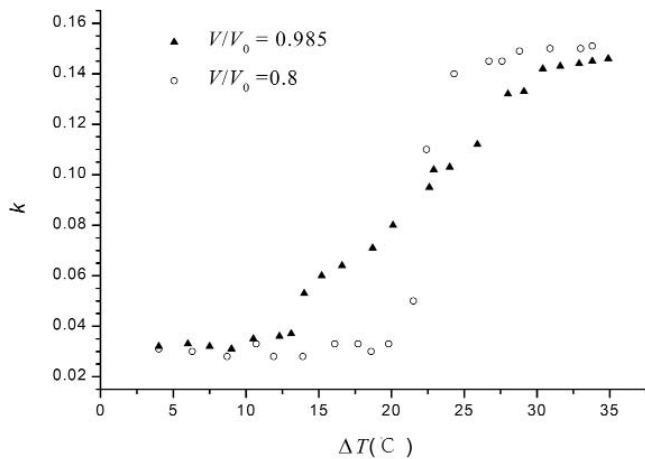


Fig. 4. Axial asymmetric degrees k versus the temperature difference ΔT for different volume ratios $V/V_0 = 0.8$ (circle marks) and $V/V_0 = 0.985$ (triangle marks).

measured. The thermocapillary convection evolved during the heating process. The velocity distributions in a horizontal cross-section at $z/\lambda = 0.25$ of the liquid bridge were measured successively by PIV, with position $z = 0$ corresponding to the bottom plane of the liquid bridge. Successive vector maps were captured at time intervals of 66 ms.

Successive frames of the velocity fields showed the bifurcation process. For the fat liquid bridge having relatively small aspect ratio, the steady and axisymmetric convection transformed to a steady and axial asymmetric convection at first. Velocity distributions were steady and axial asymmetric whenever temperature difference ΔT was kept at a certain value between 10.5°C and 34.6°C. Fig. 2 presents a typical example of a steady and axial asymmetric convection configuration in a fat liquid bridge with volume ratio $V/V_0 = 0.985$. Figs. 2(a) and 2(b), as the case of $\Delta T = 28^\circ\text{C}$, show that azimuthal velocity distributions remain the same in the time duration of 120 seconds. Fig. 3 shows the time evolution of azimuthal velocity components at positions with the same radius $r = 2.0 \text{ mm}$ but different azimuthal angles of $\theta = 90^\circ$ and $\theta = 270^\circ$ in a cross-section with temperature difference $\Delta T = 22^\circ\text{C}$. In Fig. 3, the typical uncertainty of azimuthal velocity components is about $\delta v_\theta = 0.06 \text{ mm/s}$. Azimuthal velocities at these two positions had different values, which do not change with time. Figs. 2 and 3 show that convection is in steady and axial asymmetric mode which remains unchanged over a long period of time at a certain temperature difference after the first bifurcation transition.

In a horizontal cross-section, the degree of axial asymmetric velocity distribution can be estimated by using relative maximum differences in the azimuthal velocity components at simi-

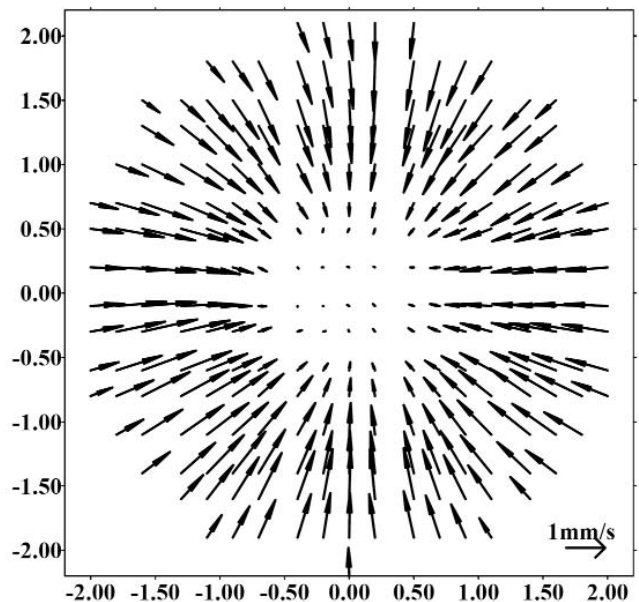


Fig. 5. A flow pattern in the horizontal cross-section ($z/\lambda = 0.25$) of a fat liquid bridge ($V/V_0 = 0.985$) when temperature difference $\Delta T = 9^\circ\text{C}$.

lar radii. The quantity k is a characteristic value that can be used to estimate axial asymmetric degree of velocity distribution

$$k = |v_{\theta_{max}} - v_{\theta_{min}}| / v_*$$

where $v_{\theta_{max}}$ and $v_{\theta_{min}}$ are, respectively, the maximum and minimum value of the azimuthal velocity components within the range between the inner diameter of 3.9 mm and the outer diameter of 4.1 mm. The typical velocity v_* is defined as $v_* = |\partial\sigma/\partial T|\Delta T_*/\rho\nu$, where ν is viscosity coefficient of the liquid and ΔT_* is a reference constant temperature difference between two solid disks. The typical velocity value corresponding to $\Delta T_* = 1$ C is $v_* = 6$ mm/s. Fig. 4 shows the experimental results of axial asymmetric degree k depending on the temperature difference in

a fat liquid bridge with volume ratio $V/V_0 = 0.985$ and in a slender liquid bridge with volume ratio $V/V_0 = 0.8$. The main sources of error in measuring velocity distributions were systematic errors. The uncertainty in each value of k in Fig. 4 is about $\delta k = 0.033$. As indicated in Fig. 4, for the case of $V/V_0 = 0.8$, k is less than or equal to δk before the onset of oscillation; then after the temperature difference raised to 21.5°C corresponding to the OTC k increases sharply to $k = 0.15$. On the other hand, in case of volume ratio $V/V_0 = 0.985$, k was always less than or equal to δk when the temperature difference was lower the certain value $(\Delta T)_{c1}$; and k increases gradually with further increase of the temperature difference ΔT before reached the other temperature difference $(\Delta T)_{c2}$ at which OTC started. As long as $(\Delta T)_{c1} \leq \Delta T \leq (\Delta T)_{c2}$, the convections appeared steady and asymmetric.

The first bifurcation is defined as $k = 0.035$ for a fat liquid bridge $V/V_0 = 0.985$, it gives

$$(\Delta T)_{c1} = 10.5 \text{ }^\circ\text{C}.$$

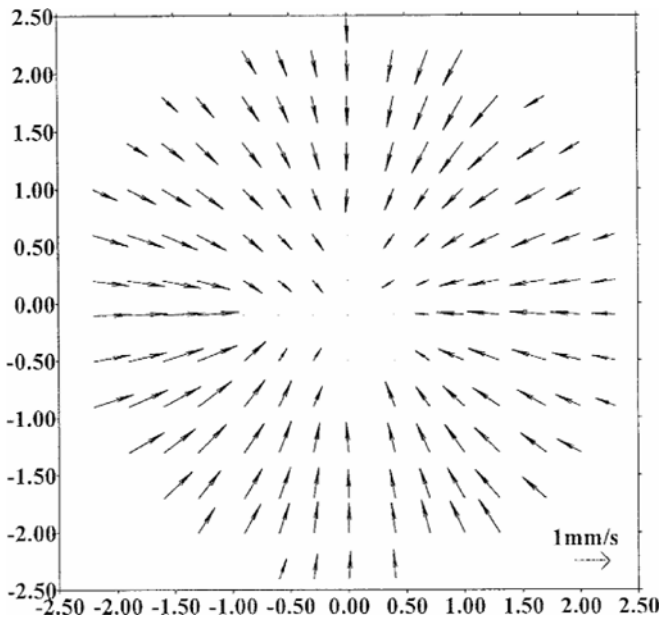


Fig. 6. Steady and axisymmetric distribution of velocity in the horizontal cross-section ($z/\lambda = 0.25$) of a slender liquid bridge ($V/V_0 = 0.8$) when temperature difference $\Delta T = 20^\circ\text{C}$.

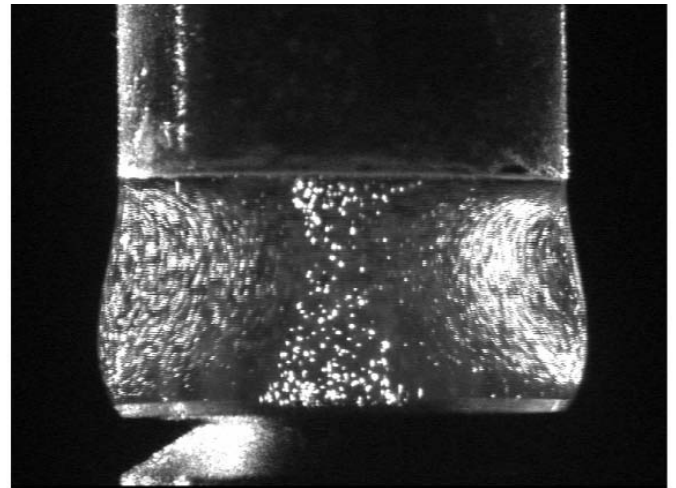


Fig. 7. A flow pattern in the vertical cross-section of a fat liquid bridge ($V/V_0 = 0.985$) when the temperature difference $\Delta T = 32^\circ\text{C}$.

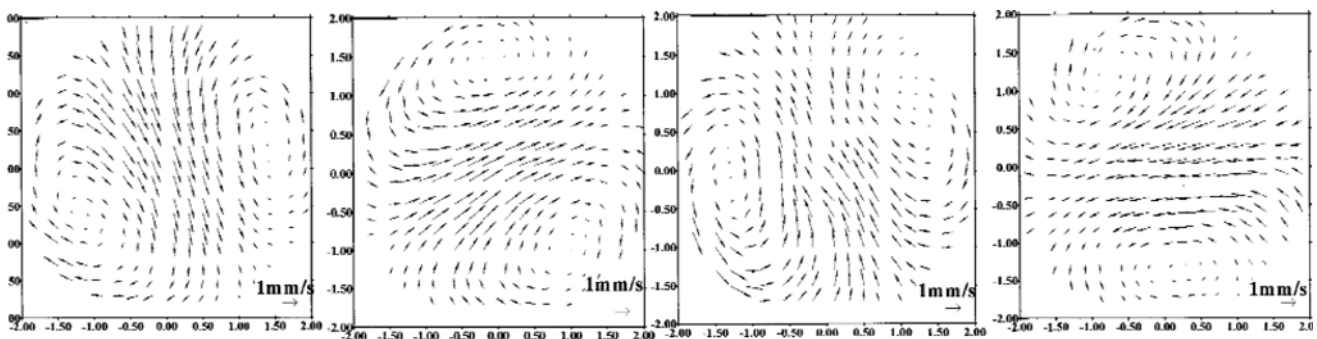


Fig. 8. Typical flow patterns in the horizontal cross-section ($z/\lambda = 0.6$) when flow is oscillating in a slender liquid bridge ($V/V_0 = 0.8$). Four sets of velocity vectors were recorded in interval of one-fourth the oscillation period.

This value is associated with the transition from steady and axisymmetric convection to the steady and axial asymmetric convection. The second critical value of the temperature difference, corresponding to the onset of OTC, is defined when the velocity distributions are observed to become time-periodic such that velocity fields oscillate, and it gives

serial number	first critical			second critical		
	T_1	T_2	$(\Delta T)_{c1}$	T_1	T_2	$(\Delta T)_{c2}$
1	23.8°C	34.3°C	10.5°C	25.7°C	60.3°C	34.6°C
2	23.6°C	34.6°C	11.0°C	25.5°C	60.2°C	34.7°C

Table 2. The temperatures of the top and bottom disks and their temperature differences at critical for two independent experiments

Volume ratio	$(\Delta T)_{c1}$	$(Ma)_{c1}$	$(\Delta T)_{c2}$	$(Ma)_{c2}$
0.7	20.8°C	3349	$(\Delta T)_{c2} = (\Delta T)_{c1}$	$(Ma)_{c2} = (Ma)_{c1}$
0.8	21.5°C	3462	$(\Delta T)_{c2} = (\Delta T)_{c1}$	$(Ma)_{c2} = (Ma)_{c1}$
0.985	10.5°C	1779	34.6°C	5861
1.06	12.1°C	2050	32.3°C	5471
1.1	13.0°C	2203	30.4°C	5151

Table 3. The critical values for different volume ratios

	Experimental results		Computational results	
height of liquid bridge	2.5 mm		5.0 mm	
diameter of liquid bridge	2.5 mm		5.0 mm	
medium	10cst silicone oil		10cst silicone oil	
volume ratios	0.8	0.985	0.8	0.985
first critical temperature difference	21.5°C	10.5°C	20.2°C	9.8°C
second critical temperature difference	21.5°C	34.6°C	20.2°C	41°C
first critical Marangoni number	3642	1779	3408	1660
second critical Marangoni number	3642	5698	3408	1946

Table 4. Comparison of the experimental results and the numerical simulation

$$(\Delta T)_{c2} = 34.6 \text{ }^\circ\text{C}.$$

The dimensionless parameter which characterizes the strength of the surface tension forces that drive the flow is the Marangoni number $Ma = |\sigma_T| \lambda \Delta T / \rho \nu \kappa$, where ν and κ are kinematic viscosity and thermal diffusivity of the liquid, the values of the fluid properties are showed in table 1. In the present experiments, the height of liquid bridge $\lambda = 2.5$, two critical values of the temperature difference correspond to two critical Maragoni numbers:

$$Ma_{c1} = 1779, Ma_{c2} = 5861.$$

Table 2 shows the reproducibility of $(\Delta T)_{c1}$ and $(\Delta T)_{c2}$ through two independent experiments under the ambient temperature around 23°C, in which, T_1 and T_2 are the temperatures of the top and bottom disks.

Although there were uncertainties $\delta k = 0.033$ in our experiments, nonetheless, the values of k were increased gradually with the temperature differences and became much larger than δk when the temperature differences were higher than first critical temperature difference $(\Delta T)_{c1}$ in a fat liquid bridge $V/V_0 = 0.985$. Axial asymmetric degree of velocity distribution could be estimated from the k value. In addition, the characteristics of flow pattern could still be displayed rather clearly. For example, for a fat liquid bridge $V/V_0 = 0.985$, Fig. 5 shows that flow pattern was axisymmetrical for temperature difference $\Delta T = 9^\circ\text{C}$, but the flow patterns in Fig. 2 show an asymmetrical feature for temperature difference $\Delta T = 28^\circ\text{C}$.

4 Transition Process in a Slender Liquid Bridge

To our knowledge, the steady and axial asymmetry convection has not been observed so far for a slender liquid bridge. Fig. 6 shows velocity distribution before OTC in a section $z/\lambda = 0.25$ at $\Delta T = 20^\circ\text{C}$ for the case $V/V_0 = 0.8$; the velocity field is steady and axisymmetric. The azimuthal velocity started to oscillate when motion became axial asymmetric. Fig. 4 indicates that k was less than or equal to $\delta k = 0.033$ before the onset of oscillation and then increasing sharply after OTC. The critical temperature differences corresponding to the onset of OTC is defined when the velocity distributions are observed to become time-periodic such that velocity fields oscillate in time, and then the critical temperature difference at the transition points are

$$(\Delta T)_{c1} = (\Delta T)_{c2} = 21.5^\circ\text{C}$$

and corresponding critical Maragoni numbers are

$$Ma_{c1} = Ma_{c2} = 3642.$$

Direct measurements of velocity distribution in a vertical cross-section should be modified due to optical distortion by lens

effect [32]. But such modification cannot be defined precisely. As an example, Fig. 7 shows the image at $\Delta T = 32^\circ\text{C}$ in a vertical cross-section. However, velocity images in a horizontal cross-section have no optical distortions and can be used to judge the critical state in case $V/V_0 = 0.985$.

5 Influence of Liquid Bridge Volume Ratio

Theoretical studies show that the critical temperature difference depends on liquid bridge volume ratio [21-23]. However, experimentally we found that for some volume ratios of the liquid bridge, successful measurement of the velocity field was hindered from the so-called "tracer particle accumulation" [33]. Velocity fields with a series of liquid bridge volume ratios were measured, but only a part of them were successful. Table 3 lists the relevant critical temperature differences for those successfully measured cases, including volume ratios $V/V_0 = 0.7$, V/V_0

$= 1.06$ and $V/V_0 = 1.1$. Results in section 3 show two bifurcation transitions in a fat liquid bridge, and only one bifurcation transition for a slender liquid bridge for a large Prandtl number fluid.

6 Flow Patterns

Measurements of the velocity distributions in a horizontal cross-section determined the onset of OTC. In a slender liquid bridge $V/V_0 = 0.8$ with an aspect ratio $A = 0.5$, OTC is a traveling wave and rotating flow state corresponding to a flow pattern $m = 1$ immediately after oscillation onset. In a fat liquid bridge $V/V_0 = 0.985$ with an aspect ratio $A = 0.5$, however, oscillatory convection appeared as a pulsating flow state related to a standing wave corresponding to a flow pattern $m = 2$; when the temperature difference was further increased, the velocity pattern started rotating and could be described as a traveling wave cor-

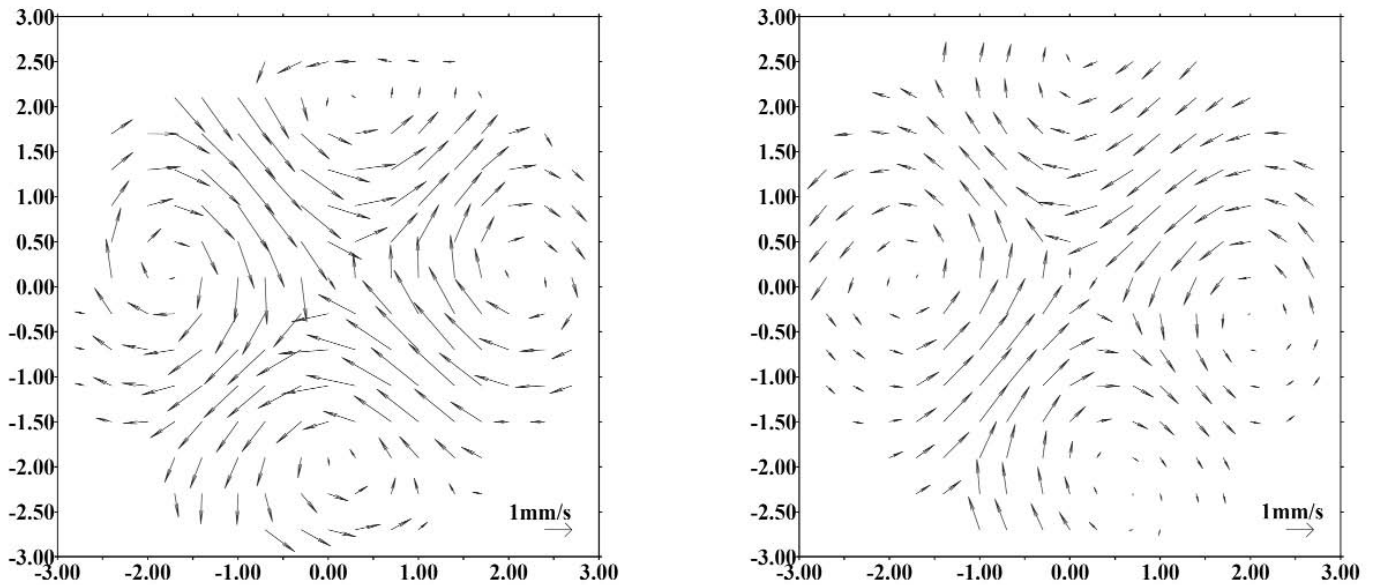


Fig. 9. Typical flow patterns (pulsating) in the horizontal cross-section ($z/\lambda = 0.6$) when flow is oscillating at temperature difference $\Delta T = 36^\circ\text{C}$ in a fat liquid bridge ($V/V_0 = 0.985$). Two sets of velocity vectors were recorded in interval of half the oscillation period.

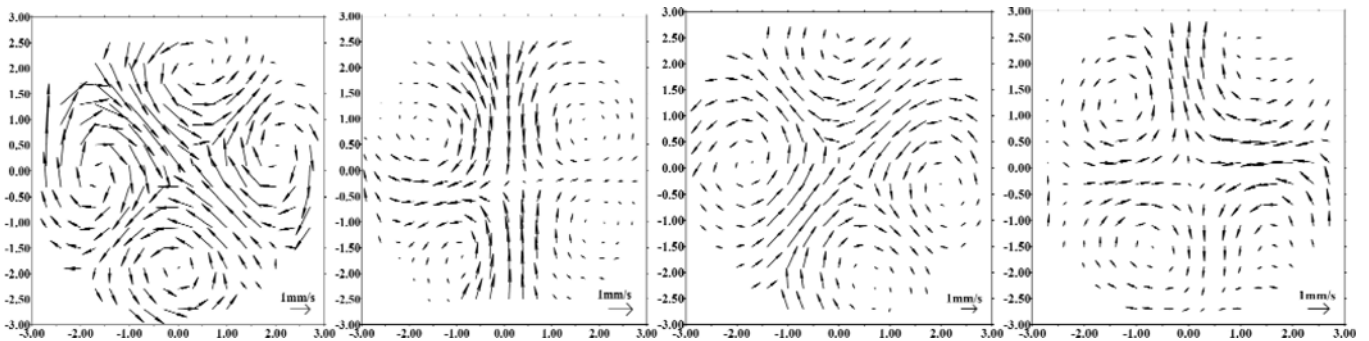


Fig. 10. Typical flow patterns (rotating) in the horizontal cross-section ($z/\lambda = 0.6$) when flow is oscillating at temperature difference $\Delta T = 38^\circ\text{C}$ in a fat liquid bridge ($V/V_0 = 0.985$). Four sets of velocity vectors were recorded in interval of one-fourth the oscillation period.

responding to a flow pattern $m = 2$ in the oscillatory regime.

Fig. 8 shows the sequence of flow patterns in one oscillatory period at $\Delta T = 23^\circ\text{C}$ in a horizontal cross-sections at $z/\lambda = 0.60$ for a slender liquid bridge $V/V_0 = 0.8$. The oscillation frequency is 0.67 Hz and oscillatory flow has a rotating instability pattern characterized by a traveling wave of $m = 1$.

Fig. 9 shows the sequence of flow patterns in one oscillatory period at temperature difference $\Delta T = 36^\circ\text{C}$ in a horizontal cross-sections at $z/\lambda = 0.60$ for a fat liquid bridge $V/V_0 = 0.985$. In this case, oscillatory frequency is 0.92 Hz and OTC has a pulsating instability pattern characterized by a standing wave of $m = 2$. Fig. 10 shows the sequence of flow patterns in one oscillatory period at temperature difference $\Delta T = 38^\circ\text{C}$ in a horizontal cross-section at $z/\lambda = 0.60$ for a fat liquid bridge $V/V_0 = 0.985$. In this case, the oscillation frequency is 1.04 Hz and the oscillatory convection has a rotating instability pattern characterized by a traveling wave of $m = 2$.

7 Comparisons with Numerical Simulation

The onset of the OCT under the Earth's gravity was investigated by the numerical method to compare with the experimental results [22-23]. In 3D numerical simulation, the floating half zone filled of 10 cst silicon oil was 5mm in diameter and 2.5mm in height. The physical properties of the fluid used in the calculation were shown in the table 1. The geometric configuration and physical parameters of the calculated liquid bridge were the same as those in the experiment. The three-dimensional, time dependent Navier-Stokes equations and temperature equation with the Boussingsq approximation were solved by the hybrid finite element method of fractional step to verify the experimental results.

The quantity k was defined as the same as in the experiment and was used to describe the asymmetric degree of velocity distribution in the transition process when temperature difference is increased. Numerical simulation results show that the onset process of the fat liquid bridge differs from that of the slender one. The OTC onset processes for both liquid bridges are described by k and the trends of k curves for both volume ratios are similar to experimental results. First critical temperature difference $(\Delta T)_{c1}$ and second critical temperature difference $(\Delta T)_{c2}$ are determined for a fat liquid bridge $V/V_0 = 0.985$ as follows:

$$(\Delta T)_{c1} = 9.8^\circ\text{C} \text{ or } Ma_{c1} = 1660$$

$$(\Delta T)_{c2} = 41.0^\circ\text{C} \text{ or } Ma_{c2} = 6946$$

Only one critical temperature differences $(\Delta T)_{c1} = (\Delta T)_{c2}$ is given for a slender liquid bridge $V/V_0 = 0.8$, that is

$$(\Delta T)_{c1} = (\Delta T)_{c2} = 20.2^\circ\text{C} \text{ or } Ma_{c1} = Ma_{c2} = 3408$$

The comparison of experimental results with the 3D numerical

ones for a fat liquid bridge $V/V_0 = 0.985$ and for a slender liquid bridge $V/V_0 = 0.8$ is shown in Table 4. For a slender liquid bridge $V/V_0 = 0.8$, the experimental result and the numerical simulation agree well. The critical Marangoni number is 3642 and 3604 obtained from the experiment and the numerical simulation, respectively, the relative difference is only 1%. For the fat liquid bridge $V/V_0 = 0.985$, the first critical Marangoni number is 1779 and 1660 for the experiment and the numerical simulation, respectively, the relative difference is 7%; the second critical Marangoni number is 5861 and 6946 for the experiment and the numerical simulation, respectively, the relative difference is 17%, and the results are in reasonable agreement. Both the experiment and the numerical simulation show that there are two critical temperature differences for fat liquid bridge $V/V_0 = 0.985$, that means there are two bifurcation transitions for thermocapillary convection of large Prandtl number fluid.

8 Conclusions

Two bifurcation transitions were observed experimentally in fat liquid bridges of a large Prandtl number, the first transition was from the steady and axisymmetric convection to the steady and axial asymmetric convection, and the second was from the steady and asymmetric convection to OTC. Similar transitions have been seen in cylindrical liquid bridge of small Prandtl numbers [19-20]. Our results agree with the results of numerical simulation and linear instability analysis [21-23].

Only one transition from a steady and axisymmetric state to OTC was observed in the slender liquid bridges $V/V_0 = 0.8$ and $A = \lambda/d_0 = 0.5$. Oscillation convection is a "rotating" flow state with mode $m = 1$. In a fat liquid bridge $V/V_0 = 0.985$ and $A = \lambda/d_0 = 0.5$, oscillation convection is a "pulsating" flow state with mode $m = 2$; when the temperature difference is increased, the oscillation convection becomes a rotating state with mode $m = 2$.

Present paper gives the experimental proof on the existence of two bifurcation processes in a floating half zone, and these results show some new features of convection in a liquid bridge with a large Prandtl number and may shed light for the understanding of the onset of oscillatory thermocapillary convection in liquid bridges, especially for a large Prandtl number fluid. It is expected that the onset of oscillatory thermocapillary convection in a large Prandtl number's liquid bridge of two bifurcation transitions is probably due to the hydrodynamic instability, similar to the one in a small Prandtl number's case as discussed in the publication of Levenstam et al. [20], but not due to the hydrothermal instability.

References

- 1 Hu, W. R., Shu, J. Z., Zhou, R. Tang, Z. M.: Influence of liquid bridge volume on the onset of oscillation in floating zone convection. I. Experiments. J. Crystal Growth vol. 142, p. 385 (1994)
- 2 Cao, Z. H., Xie, J. C., Tang, Z. M., Hu, W. R.: Experimental study on

- oscillatory thermocapillary convection. *Sci. China* vol. 35, p. 725 (1992)
- 3 Hirata, A., Sakurai, M., Ohishi, N., Koyma, M., Morita, T., Kawasaki, H.: Transition process from laminar to oscillatory Marangoni convection in a liquid bridge under normal and microgravity. *J.Jpn. Soc. Microgravity Appl.* Vol. 14, p. 137 (1997)
 - 4 Monti, R., Castagnolo, D., Dell'Aversana, P., Desiderio, G., Moreno, S., Evangelista, G.: An experimental and numerical analysis of thermocapillary flow of silicone oils in a micro-floating zone. *Proceedings of the 43rd Cong. Int. Astro. Fed., Washington, DC, 1992*
 - 5 Sumner, L. B. S., Neitzel, G. P., Fontaine, J.-P., Dell'Aversana, P.: Oscillatory thermocapillary convection in liquid bridges with highly deformed free surfaces: Experiments and energy-stability analysis. *Phys. Fluids* vol. 1, p. 107 (2001)
 - 6 Tang, Z. M, Hu, W. R.: Influence of liquid bridge volume on the onset of oscillation in floating zone convection II. Numerical simulation. *J. Crystal Growth* vol. 142, p. 385 (1994)
 - 7 Tang, Z. M, Hu, W. R.: Influence of liquid bridge volume on the onset of oscillation in floating zone convection III. Three-dimensional model. *J. Crystal Growth* vol. 207, p. 239 (1999)
 - 8 Shevtsova, V. M., Legros, J.-C.: Oscillatory convective motion in deformed liquid bridges. *Phys. Fluids* vol. 7, p. 1621 (1998)
 - 9 Chun, Ch. H.: Marangoni convection in floating zone under reduced gravity. *J. Crystal Growth* vol. 48, p. 600 (1980)
 - 10 Schwabe, D., Scharmann, A.: Some evidence for the existence and magnitude of a critical Marangoni number for the onset of oscillatory flow in crystal growth melts. *J. Crystal Growth* vol. 46, p. 125 (1979)
 - 11 Neitzel, G. P., Chang, K. T., Jankowski, D. F., Mittelmann, H. D.: Linear stability of thermocapillary convection in a model of the floating-zone crystal-growth. *Phys. Fluids A* 5, p.108 (1995)
 - 12 Wanschura, M., Shevtsova, V. M., Kuhlmann, H. C., Rath, H.: Convective instability mechanisms in thermocapillary liquid bridges. *Phys. Fluids* vol. 7, p. 912 (1995)
 - 13 Chen, G., Lizee, A. Roux, B.: Bifurcation analysis of the thermocapillary convection in cylindrical liquid bridge. *J. Crystal Growth* vol. 180, p. 638 (1997)
 - 14 Chen, Q. S., Hu, W. R.: Effect of liquid bridge volume on instability of floating half zone convection. *Intl. J. Heat and Mass Transfer* vol. 42, p. 825 (1998)
 - 15 Savino, R., Monti, R.: Oscillatory Marangoni convection in cylindrical liquid bridge. *Phys. Fluids* vol. 8, p. 2906 (1996)
 - 16 Yasuhiro, S., Sato, T., Imaishi, N.: Three dimensional oscillatory Marangoni flow in half-zone of $Pr = 1.02$ fluid. *Microgravity Sci. Technol.* Vol. 10, p. 144 (1997)
 - 17 Tang, Z. M, Hu, W. R.: A simulation model of a floating half zone. *J. Crystal Growth* vol. 192, p.335 (1998)
 - 18 Smith, M. K., Davis, S. H.: Instabilities of dynamic thermocapillary liquid layers. Part 1. Convective instability. *J. Fluid Mech.* Vol. 132, p. 119 (1983)
 - 19 Rupp, R., Mueller, G., Neumann, G.: Three-dimensional time dependent modeling of the Marangoni convection in zone melting configurations for the GaAs. *J. Crystal Growth* vol. 97, p. 34 (1989)
 - 20 Levenstam, M., Amberg, G.: Hydrodynamical instabilities of thermocapillary flow in a half-zone. *J. Fluid Mech.* Vol. 297, p. 357 (1995)
 - 21 Tang, Z. M, Hu, W. R., Imaishi, N.: Two-bifurcation transitions of the floating half zone convection in a fat liquid bridge of large Pr number. *Intl. J. Heat and Mass Transfer* vol. 44, p. 1299 (2001)
 - 22 Tang, Z. M, A.Y., Cao, Z. H., Hu, W. R.: Two bifurcation transition processes in floating half zone convection of larger Prandtl number fluid. *Acta Mechanica Sinica* vol. 4, p. 328 (2002)
 - 23 Chen, Q. S., Hu, W. R.: Instability from steady and axisymmetric to steady and symmetric floating half zone convection in a fat liquid bridge of larger Prandtl number. *Chinese Physics Letter* vol. 16, p. 822 (1999)
 - 24 Frank, S., Schwabe, D.: Temporal and spatial elements of thermocapillary convection in floating zones. *Experiments in Fluids* vol. 23 p. 234 (1997)
 - 25 Preisser, F., Schwabe, D., Scharmann, A.: Steady and oscillatory thermocapillary convection in liquid columns with free cylindrical surface. *J. Fluid Mech.* Vol. 126, p. 545 (1983)
 - 26 Velten, R., Schwabe, D., Scharmann, A.: The periodic instability of thermocapillary convection in cylindrical liquid bridges. *Phys. Fluids* vol. 3, p. 267 (1991)
 - 27 Lee, J., Lee, D. J., Lee, J. H.: On the mechanism of oscillation in a simulated floating zone. *J. Crystal Growth* vol. 152, p. 341 (1995)
 - 28 Zeng, Z., Mizuseki, H., Higashino, K., Kawazoe, Y.: Direct numerical simulation of oscillatory Marangoni convection in cylindrical liquid bridges. *J. Crystal Growth* vol. 204, p. 395 (1999)
 - 29 Lappa, M., Savino, R., Monti, R.: Three-dimensional numerical simulation of Marangoni instabilities in liquid bridges: influence of geometrical aspect ratio. *Int. J. Numer. Mech. Fluids* vol. 36, p. 53 (2001)
 - 30 Host-Madsen, A., McCluskey, D. R.: On the accuracy and reliability of PIV measurements. *Proc. of 7th Inter. Symp. on Appl. of Laser Tech. to Flow Measurement, Lisbon* (1994)
 - 31 Ar, Y., Tang, Z. M., Han, J. H., Kang, Q., Hu, W. R.: The measurement of azimuthal velocity field for oscillatory thermocapillary convection. *Microgravity Sci. Technol.* Vol. 10, p. 129 (1997)
 - 32 Lan, C. W., Kou, S.: Formulation for correcting optical distortions due to a transparent floating zone. *J. Crystal Growth* vol. 132, p. 471 (1993)
 - 33 Schwabe, D., Hintz, P., Frank, S.: New features of thermocapillary convection in floating zones revealed by tracer particle accumulation structures (PAS), *Microgravity Sci. Technol.*, Vol. 9, p.163 (1996)